

A Direct Method of Studying Adsorption of a Surfactant at Solid–Liquid Interfaces

H. Haidara,[‡] M. K. Chaudhury,^{*,‡} and M. J. Owen

Dow Corning Corporation, Midland, Michigan 48686

Received: January 4, 1995[⊗]

A self-assembled monolayer of decyltrichlorosilane ($\text{Cl}_3\text{Si}(\text{CH}_2)_9\text{CH}_3$) supported on elastomeric polydimethylsiloxane (PDMS) was used as a model system to study the adsorption of a nonionic surfactant [$\text{H}(\text{CH}_2)_{12}(\text{OCH}_2\text{CH}_2)_7\text{OH}$] at the solid–liquid interface. The deformation produced on contacting a semispherical lens of the elastomer with a flat sheet under water varied systematically in response to the amount of surfactant added to the aqueous phase. The JKR theory of contact deformation in conjunction with the Gibbs' theory of interfacial thermodynamics yielded the required interfacial tension and surface excess quantities at solid–liquid interface.

Introduction

Thermodynamic analysis of the adsorption of surfactant at a liquid–air interface can be done using Gibbs adsorption equation:¹

$$\Gamma = -(C/RT)(\partial\gamma/\partial C) \quad (1)$$

where, Γ is the surface excess of the adsorbed surfactant, C is the concentration of the surfactant in the solution, γ is the surface tension at the liquid–air interface, and R and T are the molar gas constant and temperature, respectively.

By contrast, estimation of the surface excess quantities at the solid–liquid interface is not that straightforward because its interfacial tension is not readily measurable. The relevant surface excess quantities, in this case, are therefore obtained by spectroscopic and weight gain methods.^{2–5} Here we report a study where the interfacial tension of a solid–solution interface could be measured directly as a function of the bulk concentration of a surfactant, thus allowing a direct estimate of Γ_{sl} from the Gibbs adsorption equation (eq 1).

The method of determining the interfacial tension is based upon measuring the deformation produced on bridging a semispherical elastomer of polydimethylsiloxane (PDMS) in contact with another flat sheet under aqueous solutions of a nonionic surfactant [$\text{H}(\text{CH}_2)_{12}(\text{OCH}_2\text{CH}_2)_7\text{OH}$]. Using the theory of Johnson, Kendall, and Roberts (JKR),⁶ the interfacial tension γ_{sl} is calculated from the radius (a) of contact deformation at zero load according to the equation:

$$\gamma_{\text{sl}} = Ka^3/12\pi R^2 \quad (2)$$

where K is the composite modulus and R is the radius of the semisphere. Johnson et al.⁶ used the method of contact deformation to measure the interfacial tension of a surfactant solution/rubber interface. Later, using the same basic principles, Pashley et al.⁷ estimated the interfacial tension of a surfactant coated mica and water, and Chaudhury and Whitesides⁸ measured the interfacial tension of a silicone rubber and

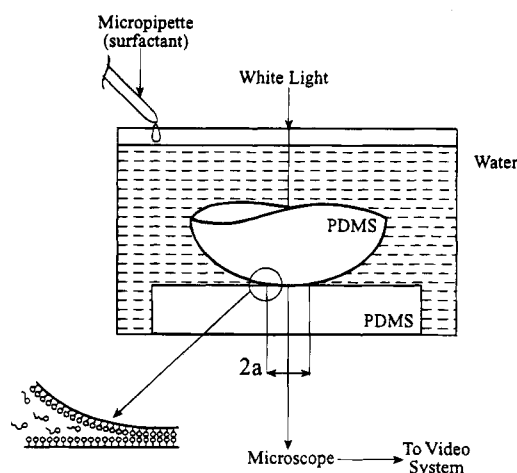


Figure 1. Schematic view of the experimental set-up showing the contact deformation produced on bridging a semispherical PDMS lens into contact with a PDMS flat sheet. Both the lens and flat sheets are modified with decylsiloxane monolayers. The contact region around the annular region is magnified in order to show the local structure of the chemisorbed decylsiloxane monolayer and surfactant molecules in water.

solutions of water and methanol. This method was also recently by Sharma et al.⁹ to measure the interfacial tension of a self-assembled silane monolayer and water.

In our current studies, the surface of polydimethylsiloxane was modified by a self-assembled monolayer of decylsiloxane according to a method described earlier.^{8,10,11} Silane modified PDMS surface is hydrophobic ($\theta_{\text{water}} = 112^\circ$) as well as oleophobic ($\theta_{\text{hexadecane}} = 42^\circ$). Furthermore, it provides a chemically homogeneous surface as evidenced by the relatively low contact angle hysteresis (ca. 8°) of water. The contact deformation experiments were performed by first bringing small semispherical lenses of PDMS into contact with flat sheets of PDMS under water and then injecting the surfactant [$\text{H}(\text{CH}_2)_{12}(\text{OCH}_2\text{CH}_2)_7\text{OH}$] in the aqueous subphase (Figure 1). Followed by the addition of surfactant, the area of contact at first decreases and then reaches an equilibrium value. The magnitude of the contact deformation at equilibrium varied systematically as a function of the concentrations of the surfactant. These contact deformations in conjunction with the JKR (eq 2) and Gibbs (eq 1) equations allowed estimation of Γ_{sl} at the polymer–water interface.

[†] On leave from Laboratoire de Physico-Chimie des Surfaces Solides, CNRS, 24 Ave. Kennedy, 68200 Mulhouse, France.

[‡] Current address: Department of Chemical Engineering, Lehigh University, Bethlehem, PA 18015.

* To whom correspondence should be addressed.

[⊗] Abstract published in *Advance ACS Abstracts*, April 15, 1995.

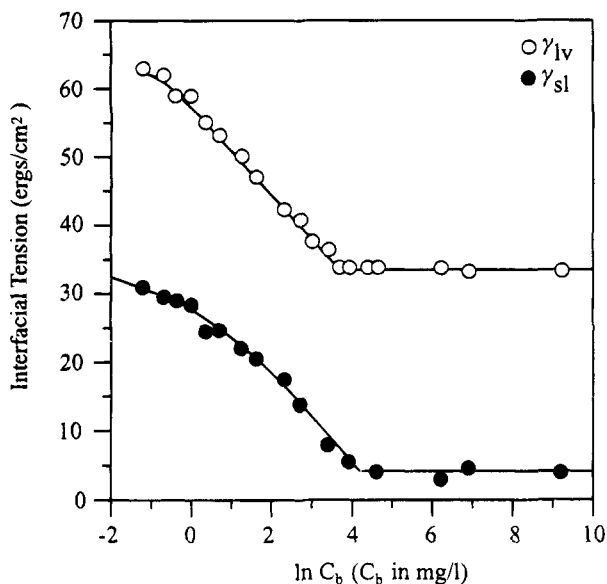


Figure 2. Gibbs plot of the interfacial tension γ versus $\ln(C_b)$ at 23 °C. C_b (mg/mL) is the bulk concentration of the surfactant (heptaethylene glycol mono-*n*-dodecyl ether) in water. The open circles represent the adsorption at the liquid–air interface and the closed circles represent the adsorption at the solid–liquid interface.

Results and Discussion

The surface tensions of the aqueous solutions of the surfactant were measured in air using the Wilhelmy plate method. The corresponding Gibbs plot of γ_{lv} versus $\ln C_b$ is shown in Figure 2. This plot shows a clear break at $\ln C_b = 3.7$, giving a value of the critical micellar concentration (cmc) of the surfactant as 8.1×10^{-5} M/L. The surface excess Γ_{lv} of the adsorbed surfactant at liquid–vapor interface, estimated from the linear portion of the plot, is 2.7×10^{-10} mol/cm² giving the corresponding molecular area (σ_{lv}) of the adsorbed surfactant as 61 \AA^2 . These values of Γ_{lv} and σ_{lv} are somewhat different from the corresponding values¹² ($\Gamma_{lv} = 3.6 \times 10^{-10}$ mol/cm²; $\sigma_{lv} = 46 \text{ \AA}^2$), measured at 55 °C.

The results of the contact deformation experiments under aqueous solutions of the surfactant are summarized in Figure 4. When the surfactant is added to water, the contact area decreases after a brief induction period (1 to 3 min). In Figure 4, the decrease of the interfacial tension is shown by plotting $\gamma_{sl}(t)/\gamma_{sl}(0)$ versus time (t). According to the arguments of fracture mechanics,¹³ the stability of contact of a sphere on a flat plate is determined by the balance of the tensile stresses at the edge due to adhesion and the crack closing stresses resulting from the intermolecular forces present in the open surfaces of the crack. Adsorption of surfactant on the open surfaces reduces their attraction, causing the crack to open further and driving the interface to a new mechanical equilibrium. Since the polymer used here is elastic, it is reasonable to assume that the crack opens up instantaneously. Although, we have not proven the above hypothesis by direct measurement of crack speed, the time scale of crack propagation (less than a second), in experiments where change of contact area is induced by external loads, is much faster than what (minutes) is seen in the current experiments. The crack growth, thus, is expected to be in equilibrium with the local concentration of the surfactant. Although we have not analyzed these data in any detail, it is reasonable to expect that the kinetics of crack propagation, to a large extent, is limited by the bulk diffusion of surfactant. Recently, Parker and Rutland¹⁴ studied the time-dependent adhesion between glass surfaces in a dilute surfactant solution, while keeping the surfaces in contact for different amounts of

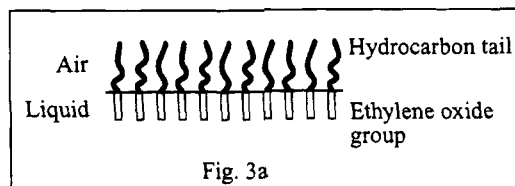


Fig. 3a

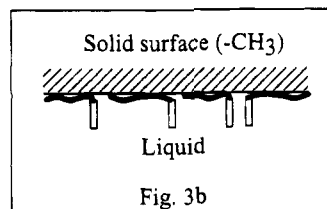


Fig. 3b

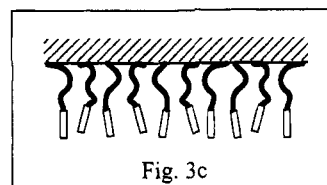


Fig. 3c

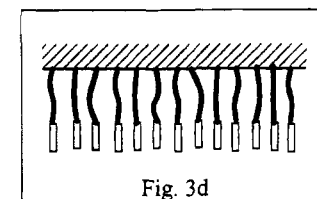


Fig. 3d

Figure 3. Hypothetical adsorption scheme and structure of the adsorbed surfactant at the liquid–air interface (a) and at the solid–liquid interfaces (3b–d): (b) low bulk concentration of the surfactant; (c) medium concentration of the surfactant, and (d) surface saturation. This simple scheme does not invoke the possibility of the adsorption of surfactants as clusters, which may very well be the case; however, our experimental results cannot distinguish the possibility of cluster formation from that of homogeneous adsorption.

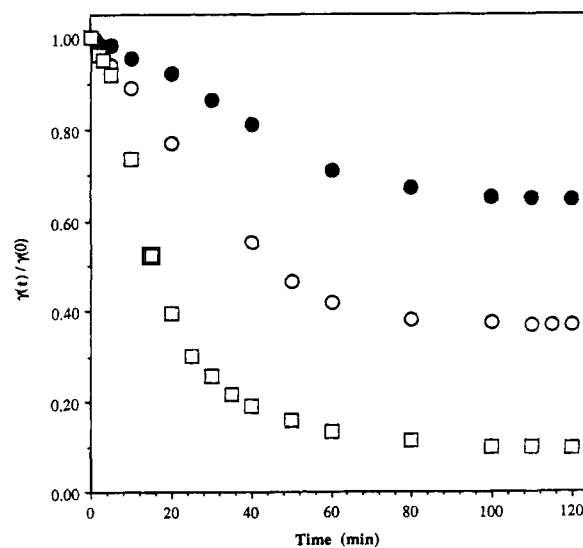


Figure 4. Kinetics of surfactant induced debonding of the solid–solid interface. The dimensionless interfacial tension $\gamma_{sl}(t)/\gamma_{sl}(0)$, which corresponds to the function $a^3(t)/a^3(0)$, is plotted as a function of time (t) for different surfactant concentrations C_b (mg/mL): (●) $C_b = 1$, (○) $C_b = 10$, (□) $C_b = 10^3$.

time. Since the surfactant increases the hydrophobicity of the glass/water interface, the adhesion increased with time following

$t^{1/2}$ kinetics, which was interpreted by the authors as evidence for a diffusion-controlled adsorption.

At large time ($t > 100$ min), the interfacial tensions reached constant values, which were used for Gibbs analysis. The equilibrium values of the interfacial tensions were calculated according to eq 2. The corresponding Gibbs plot is shown in Figure 2, which is compared with the Gibbs plot obtained at the liquid-air interface. The two adsorption isotherms exhibit somewhat different behavior over a wide range of bulk concentration below the cmc. While the isotherm at the liquid-air interface is linear below the cmc, significant curvature is seen for the corresponding isotherm at the liquid-solid interface. These results suggest some qualitative differences in the adsorption scheme of the surfactant at liquid-air and liquid-solid interfaces. In the region of very low bulk concentration (from $C_b = 0$ to $C_b = 2 \times 10^{-6}$ mol/L), the molecular area determined from an average surface excess of $\Gamma_{sl} = 8.8 \times 10^{-11}$ mol/cm² is $\sigma_{sl} = 188 \text{ \AA}^2$. The molecular area in the medium range of concentration is 98 \AA^2 , while its value is about 53 \AA^2 close to the cmc. We surmise that the differences in the adsorption patterns at air-water and polymer-water interfaces are due to the following reasons. While, the hydrocarbon tails of the adsorbed surfactant can protrude out of water and self-assemble in the air phase, they are constrained to do so at the solid-liquid interface (Figure 3). The large molecular surface area ($\sigma = 188 \text{ \AA}^2$) at low surfactant concentration indicates that the hydrophobic part of the surfactant lies along the surface of the impenetrable hydrophobic solid surface or that the molecules adsorb as loosely packed clusters. As the concentration is increased, the clusters either grow in size or the lateral hydrophobic interaction brings the "gaseous" adsorbed molecules much closer, promoting further adsorption in the free space.

At concentrations close to the cmc, increased later hydrophobic attraction leads to a more densely packed self-assembled structure of the adsorbed surfactant. It should be noted that, at surface saturation, the average area per molecule of the adsorbed surfactant at the polymer-water interface (53 \AA^2) is slightly lower than that (61 \AA^2) at the air-water interface, indicating that the surfactant is slightly more packed at the polymer-water interface. This difference is expected, because the extra van der Waals interaction between the alkyl chains of the surfactant and the polymer surface somewhat lowers the free energy required for the surfactant to self-assemble at the polymer-water interface than at the air-water interface.

Concluding Remarks

We have shown that the method of contact mechanics, as developed by Johnson, Kendall, and Roberts, can be used to study adsorption of surfactant at the solid-state interface. This study indicates that the adsorption of surfactant at solid-liquid interface occurs in a more gradual manner than is the case with air-liquid interface. The crack opening in the surfactant solution may be controlled by the diffusion of the surfactant, but this aspect has not been analyzed here. The surfactant induced debonding may provide a useful method to study the dynamics of crack propagation in other related systems.

Experimental Section

Materials. The plasma oxidation was carried out in a Harrick Plasma Cleaner (Model PDC-23G, 100 W). The silane was purchased from Petrach. The water used in these studies was purified using a Nanopure water purifier (Barnstead) and has a surface tension of 72.7 dyn/cm. The surfactant (heptaethylene glycol mono-*n*-dodecyl ether) was purchased from Nikko Chemicals Co., Ltd. (Tokyo, Japan) and used without further purification. The contact radii $a(t)$ were measured using an inverted microscope (Nikon, Daphot), which was equipped with a video camera and a video recorder. The surface tensions of the aqueous solutions of the surfactant were determined using a Cahn automatic electrobalance (DCA 312).

Methods. The PDMS elastomers were prepared from the clear components of Dow Corning Sylgard-170A and 170B at proportions of 1:3. The surfaces of PDMS elastomers were modified by first exposing them to an oxygen plasma (45 s, 0.2 Torr) to generate a thin superficial oxide layer, which was derivatized by reacting it with the vapor of decyltrichlorosilane under reduced pressure. The details of the surface modification are described in refs 8, 10, and 11. The experimental cell (a polystyrene petri dish) contained a known volume (V_1) of water, in which the initial contact between the semisphere and flat sheet was made. The final volume of solution was adjusted to 40 mL by injecting a weighted volume ($40 - V_1$) of a surfactant stock solution to meet the desired final bulk concentration C_b . After a short induction time, the contact area started to decrease and finally reached an equilibrium value. The contact areas were recorded in a video recorder and analyzed at leisure. Surface tensions at the liquid-air interface were measured at $23^\circ (\pm 0.5^\circ)$ and a constant speed ($5 \mu\text{m/s}$) of immersion of the platinum plate. The mean standard deviations corresponding to these experimental data are 0.5 erg/cm^2 for γ_{lv} and 1 erg/cm^2 for γ_{sl} .

Acknowledgment. M.K.C. wishes to thank Dr. M. Rutland for valuable discussions.

References and Notes

- (1) Adamson, A. W. *Physical Chemistry of Surfaces*, 3rd ed.; John Wiley: New York, 1976.
- (2) Somasundaran, P.; Kunjappu, J. T. *Colloids Surf.* **1989**, *37*, 245.
- (3) Sarkar, D.; Chattoraj, D. K. *J. Colloid Interface Sci.* **1993**, *157*, 219.
- (4) Caminati, C.; Gabrielli, G. *Colloids Surf. A: Physicochem. Eng. Aspects* **1993**, *70*, 1.
- (5) Milton, J. R. *Surfactant and Interfacial Phenomena*, 2nd ed.; Wiley: New York, 1989.
- (6) Johnson, K.; Kendall, K.; Roberts, A. D. *Proc. R. Soc. London, A* **1971**, *324*, 301.
- (7) Pashley, R. M.; Israelachvili, J. N. *Colloids Surf.* **1981**, *2*, 169.
- (8) Pashley, R. M.; McGuiggan, P. M.; Horn, R. G.; Ninham, B. W. *J. Colloid Interface Sci.* **1988**, *126*, 569.
- (9) Chaudhury, M. K.; Whitesides, G. M. *Langmuir* **1991**, *7*, 1013.
- (10) Wood, J.; Sharma, R. *Langmuir* **1994**, *10*, 2307.
- (11) Chaudhury, M. K.; Whitesides, G. M. *Science* **1992**, *255*, 1230.
- (12) Chaudhury, M. K.; Owen, M. J. *J. Phys. Chem.* **1993**, *97*, 5722.
- (13) Schick, M. J. *J. Colloid Sci.* **1962**, *17*, 801.
- (14) Maugis, D. J. *Colloid Interface Sci.* **1992**, *150*, 243.
- (15) Parker, J. L.; Rutland, M. W. *Langmuir* **1993**, *9*, 1965.